CONSTRUCTION OF CNFY-CNF1 CHIMERA PROTEIN FOR STUDY OF DIFFERENTIAL PH DEPENDENT ACTIVITY OF CNF PROTEINS

BY

PHILEMON HUEI-HAN CHAN

THESIS

Submitted in partial fulfillment of the requirements
for the degree of Master of Science in Biology
in the Graduate College of the
University of Illinois at Urbana-Champaign, 2014

Urbana, Illinois

Advisor:

Professor Brenda Anne Wilson

Abstract

In this thesis we will explore the topic of cytotoxic necrotizing factors (CNFs) and show the creation of chimeric constructs to further test the details of CNF translocation into the cell. The CNF family of toxins is under the larger family of dermonecrotic AB toxins. These AB toxins have the ability to cause dermonecrosis when applied to the skin of animals. Among the dermonecrotic toxins, *Pasteurella multocida* toxin (PMT) and cytotoxic necrotizing factors 1, 2, and Y (CNF1, 2, and Y) are of interest. PMT, CNF1, CNF2, and CNFY are closely related in amino acid sequence. In a previous study on PMT, the method of translocation of the toxin into the cell for the release of the active domain was studied. Results showed that PMT enters the cell through back-trafficking in the endosomal pathway. It was also found that CNFs follow this same pathway into the cell. Interestingly, CNF1 and CNF2 were found to behave with increased efficiency of translocation across the endosomes when subjected to low levels of the inhibitors bafilomycin A1 (BafA1) and ammonium chloride (NH_4Cl) compared with CNFY and PMT. A sequence comparison showed that CNF1 and CNF2 have higher pI in a specific region on the translocation domain than that of CNFY and PMT; a probable cause of the difference in translocation under low inhibitor levels. This being so, an experiment to specifically isolate and test the differences in activity caused by the translocation region was proposed. Chimeric CNF constructs involving variable translocation domains among the CNFs with constant activity domain and vice versa are proposed. In this thesis we specifically discuss the construction of the CNFY1 chimera from CNFY translocation domain and CNF1 activity domain. Generation of this chimera provides a foundation for additional constructs, as well as direction to begin testing. Using serum response element (SRE) has been seen as an effective way to test cellular activity for PMT and CNFs. In this thesis, we focus on the construction of CNF chimeras so that SRE-based reporter tests may be conducted in future studies.

Acknowledgements

I would like to thank my advisor Dr. Brenda Wilson for the guidance and direction provided during the entire process, not only in the laboratory setting but also in life skills outside of research.

I would like to thank Dr. Mengfei Ho for his patience and teaching in the lab, sharing his insight and technical expertise.

I want to thank all the members of the Wilson lab for their encouraging words and upbeat attitude, making this lab an enjoyable place to work.

I would like to thank Dr. Joanna Shisler for her guidance as the second reader for my thesis.

I would like to thank the friends and family that supported me both financially and emotionally through this process.

Table of Contents

Chapter 1: Introduction

1.1 Bacterial Toxins

Bacteria have found many different ways to increase virulence within hosts. Pathogenicity factors, such as antibiotic resistance, cell wall modification, and secreted exotoxins, increase survivability of the pathogen within the host. An exotoxin is a poisonous substance made and secreted by bacteria into its surrounding medium. They are usually produced inside the pathogen and are secreted outside the bacterial membrane through various secretion pathways and then bind to and affect the host target cells. Despite its detrimental effects, it is possible to use the toxin mechanisms for beneficial purposes. The transmembrane transport system is naturally used for mobilizing toxin catalytic domains, but it may be possible to use the same transport to carry other desired chemicals or proteins as cargo for delivery into cells. In making these chimeric proteins, hormones and other chemicals can have very specific targeting to cells through their receptor-binding domains. It could also be possible to alter the binding and transmembrane portions of the toxin to modify the target cell or receptor specificity. This is very powerful in regulating downstream effects in a multisystem organism such as an animal or human. There has been a successful attempt to create a drug specifically targeting lymphoma cells that express CD25 using chimeric "fusion" proteins based on toxins [1]. This would be a possible route to explore after more depth of inquiry has been done on toxin targeting, translocation, and catalysis.

1.2 Exotoxins

There are three types of exotoxins that are classified by their method of application. Type I toxins are characterized by their ability to hyperactivate host defenses. Known as superantigens, these proteins stimulate inflammation in the host by profusely binding to T4 lymphocytes and antigen-presenting cells, causing the abundant release of cytokines such as interleukin-2. Excess amounts of cytokines circulating in the blood stream cause endothelial damage, shock, intravascular coagulation, and organ failure. Type II toxins are characterized by the ability to form pores in the target membranes and/or damage the membrane. Pores are formed by some Type II toxins protein insertions into the target membrane, while other membrane-damaging effects come from phospholipase toxins that degrade membrane molecules. Very often

1

they are necrotic in nature, leaving dead flesh in the affected area. Type III toxins are known as AB toxins. AB toxins have two parts to the protein. There is generally a binding and/or translocation domain (B part) and a catalytic domain (A part). Entry of the AB toxin into the host cell occurs first by binding of the B domain to a surface receptor of the host cell. This triggers one of two events depending on the nature of the toxin. Either the toxin-receptor complex is phagocytosed into the cell and the A domain released into the cytosol, or the A domain is directly translocated across the phospholipid bilayer by the B part. The exact mechanism for translocation across the membrane has not yet been elucidated and further studies are being conducted. If the toxin receptor complex is phagocytized, the vesicle then fuses with the endosome. From this point, there are a variety of methods that the A domain uses to escape into the cytosol. In one of these pathways, the endosome acidifies, causing the A domain to translocate across the membrane and be released into the cytosol. Other toxins such as ricin toxin (RT) and cholera toxin (CT) are trafficked through the Golgi into the ER where they enter the cytosol. Finally, toxins can also move into the cytosol from the recycling endosome as seen in *Pseudomonas* exotoxin (PE) [2, 3]. Once in the cytosol many A domains, such as with CT and CNF (cytotoxic necrotic factor), will enzymatically modify G-proteins causing them to be constitutively active.

1.3 G-Proteins

G-proteins are a major part of host cell signaling. Many of them are coupled with a G-protein coupled receptor (GPCR) that resides on the cell membrane to receive extracellular signals. GPCRs are membrane bound proteins that serve as a signal relay from extracellular to intracellular signals. They are made up of seven transmembrane alpha helices linked to an extracellular receptor. The cytosolic side is bound to a G-protein. When a ligand binds to the receptor the GPCR changes conformation and acts as a guanine nucleotide exchange factor (GEF) for the G-protein [4]. G-proteins act as the start of a signaling pathway that activates downstream activities. G-proteins start with GDP bound to them. Upon stimulation by the GEF, the alpha subunit releases bound GDP and binds GTP. When activated by a substrate, the GDP is exchanged for a GTP to activate the G-protein, and then the G-protein binds to the target molecule to activate it. GTP is hydrolyzed back to GDP and the G-protein converts back to its inactive state. The activated target molecule then continues the signal cascade downstream.

G-proteins can be monomeric or heterotrimeric. Heterotrimeric G-proteins have alpha, beta, and gamma subunits. The alpha subunit is about 45-47 kDa, the beta subunit 35 kDa, and the gamma subunit 7-9 kDa. The alpha, beta, and gamma subunits are linked together and bound to the GPCR. This allows the beta-gamma complex to disassociate [5]. The beta-gamma complex activates different signaling cascades before returning to the alpha subunit. The alpha subunit is a GTPase that hydrolyzes GTP to GDP and rebinds to the beta-gamma subunit. Monomeric G-protein is formed from a single protein chain. There are many families and classes of monomeric G-proteins. Many of these G-proteins are themselves modified by other proteins. Due to the tight binding of GDP and slow hydrolysis of GTP on these small G-proteins, they are enzymatically augmented by other proteins [6]. GEF disassociates GDP from the protein and GTPase activating protein (GAP) facilitates hydrolysis of GTP to GDP. These two proteins are part of a cycle in activation and deactivation of monomeric G-proteins. Monomeric G-proteins not only have the ability to interact with regulatory proteins, they also interact among themselves, switching processes on and off. Their size ranges from 20 to 40 kDa and their downstream effects are very diverse. Families such as Rho and Rac GTPases participate in regulation of the actin cytoskeleton. Other families such as SAPK and MEK regulate transcription and translation signaling in the cell [7].

1.4 Toxins Affecting G-Protein Pathways

Many toxins produced by pathogenic bacteria modify G-protein function during infection. Toxins that affect G-protein pathways usually do so by modifying certain regulatory proteins in this pathway, making them constitutively active or inactive. This has compounding effects because the signaling cascade is usually amplified as it proceeds downstream. Constitutive activity easily perturbs homeostasis. For example, toxins that activate $G\alpha_s$ cause activation of acetylate cyclase, which in turn produces cAMP. This causes a large outflow of ions and water from the cell, which in intestines results in diarrhea. CNF1 modifies RhoA GTPase by deamidating the glutamine in the active site at position 63, causing it to be constitutively active and stimulate actin polymerization [8]. Actin is a monomeric protein molecule that polymerizes in a double helix to form fibers. The fibers associate with each other to form actin bundles or actin networks. Bundles are formed by parallel running fibers while networks are fibers that run orthogonal to each other. Under normal situations the fibers provide

a stable structure and allows for movement of the cell surface. Constitutively active RhoA will cause rapid formation of actin stress fibers and change the shape of the cell. CNF2 also performs similar actions on RhoA; however, the targeted cells differ slightly from CNF1 toxins [9]. (Figure 1.1)
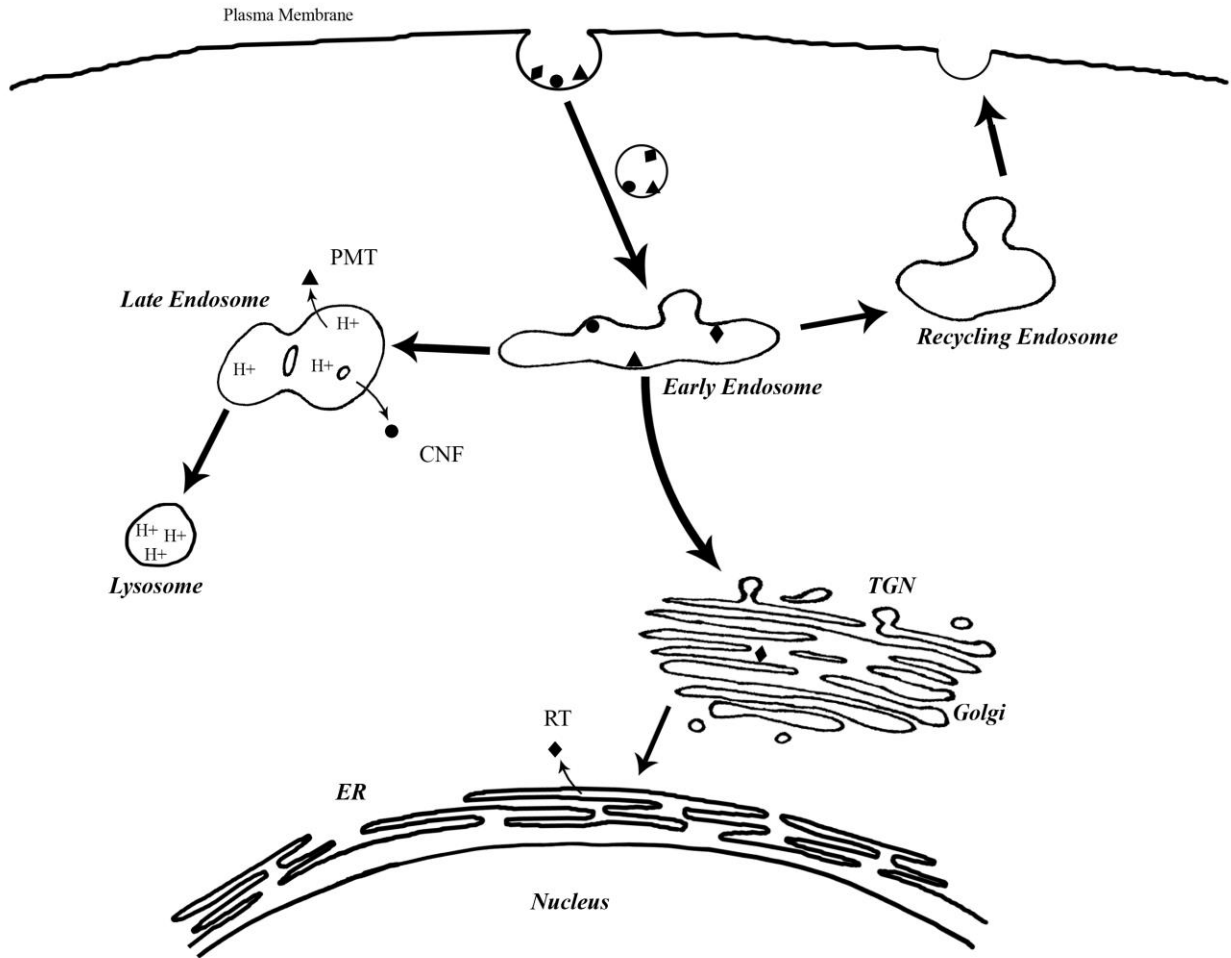
Figure 1.1
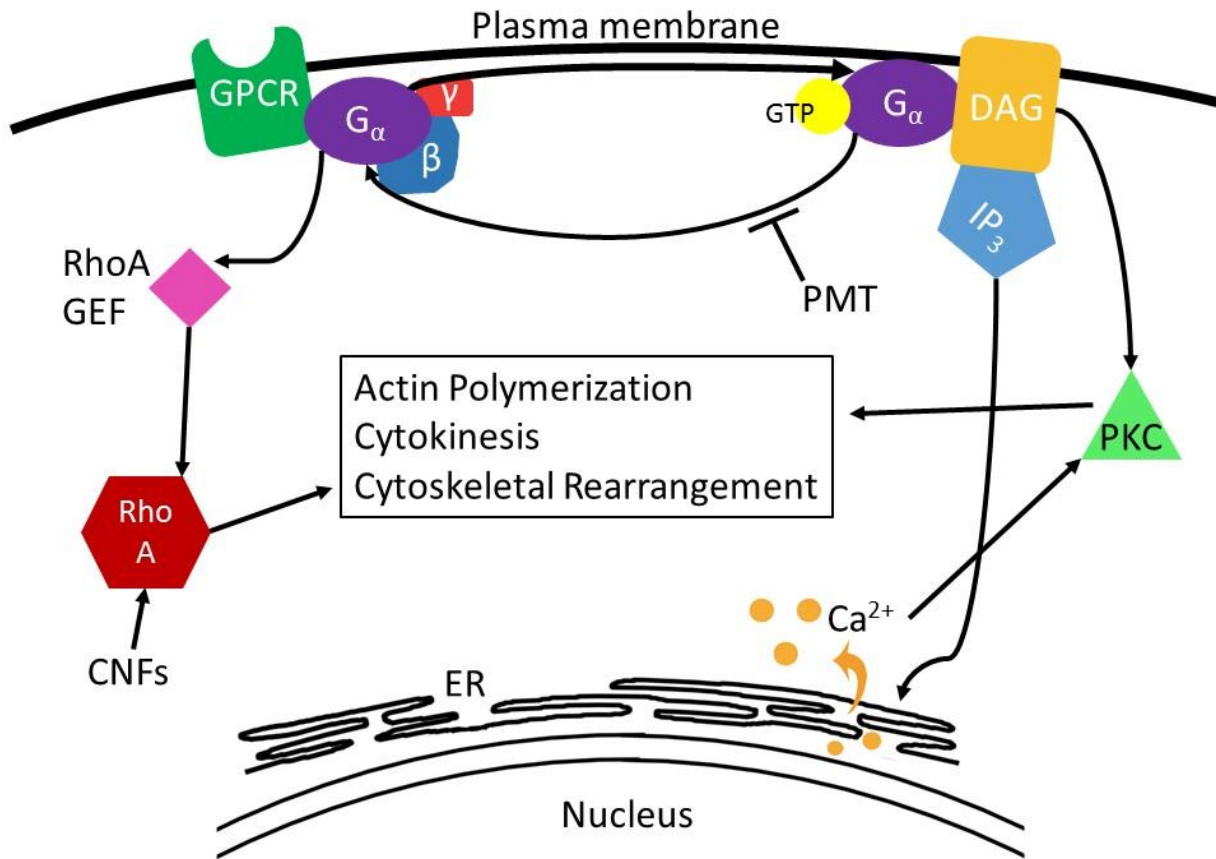
Toxins act on the G-protein signaling cascade: This simplified diagram shows toxin action on G-protein pathways and the downstream signals. Cytoskeletal rearrangement can be achieved through a variety of different paths, either through PKC activation or RhoA activation. PMT locks Gα in the active conformation to increase downstream signaling. CNF family toxins lock RhoA in the active formation to increase downstream signaling.

1.5 Looking at Membrane Translocation

The translocation of the active domain across the membrane into the cytosol of the host is only partly understood. Studies have been made to see where along the endosomal pathway translocation occurs. While the timing and conditions of translocation are better known, the exact molecular mechanism is still being studied. One pathway involves uptake and trafficking to the Golgi apparatus and subsequent translocation. The pathway starts with toxin binding to receptors at the host membrane followed by endocytosis. Some toxins such as PMT will bind to the membrane itself for cell uptake [10]. Toxins such as CNF1 and CNF2 bind to the laminin receptor precursor (LRP) for endocytosis [11].Endocytosis can be either clathrin-dependent or clathrin-independent. Vacuoles all converge at the endosome following endocytosis. From the endosome, some toxins are trafficked to the trans-Golgi network (TGN). From the TGN, some toxins are further trafficked to the ER membrane where they use the native protein channels to access the cytosol [12]. Ricin toxin uses this method to achieve entry into the cytosol. Ricin is a naturally occurring AB toxin found in the seed of the castor oil plant *Ricinus communis* [3].

The alternate pathway for toxin translocation into the cytosol from the endosome uses the acidification process of the endosome. Toxins that use this pathway bind to the native receptors on the host cell and are ingested via clathrin-mediated phagocytosis or clathrin-independent phagocytosis. Similar to before, the phagosome is fused with the endosome. Once merged, acidification of the endosome causes insertion of the translocation domain into the membrane, forming a pore that mediates transfer of the catalytic domain into the cytosol [13]. The A part of the toxin is then translocated across the membrane into the cytosol and released in the cytosol. Notable toxins that follow this pathway are diphtheria toxin and botulinum neurotoxins [14, 15]. PMT, and CNFs 1, 2, 3 and y also follow this pathway [16, 17, 18]. (Figure 1.2)

Figure 1.2

Plasma Membrane

PMT

Late Endosome

H+

H+   H+

CNF

Lysosome

H+   H+
H+

Early Endosome

Recycling Endosome

TGN

Golgi

RT

ER

Nucleus

Many toxins utilize the endosomal pathway for infection: The toxins are phagocytosed and incorporated into the early endosome. Here ricin toxin (RT) continues on through the trans-Golgi network and is trafficked into the ER where it is released into the cytoplasm. PMT and toxins from the CNF family traffic to the endosome and translocate the activity domains across the endosomal membrane upon acidification.

1.6 *Pasteurella multocida* Toxin (PMT)

In a previous study, PMT (*Pasteurella multocida* toxin) translocation of the activity domain into the cell was studied [19]. PMT causes atrophic rhinitis in pigs and inflammation in humans. In most animals, the effects of *Pasteurella multocida* infection include but are not limited to hepatic necrosis, nasal and splenic atrophy, pneumonia symptoms and even death [20]. PMT uses the endosomal pathway for uptake into the cell. Host cell binding requires an abundance of sphingomyelin and possibly a protein co-receptor [10]. After endocytosis, PMT is trafficked to the late endosome and consequently translocates across the membrane as the pH is lowered [16]. PMT indirectly affects the RhoA pathway through deamidation of $G_{\alpha q}$ causing it to lose GTPase activity and become constitutively active [21] [22].

1.7 Cytotoxic Necrotizing Factor 1 (CNF1)

The CNF toxins are secreted toxins, or exotoxins, produced by pathogenic strains of *Escherichia coli* [23]. The CNF toxins, like PMT, are classified as Type III toxins. CNF 1 also causes disease in humans as a result of infection with uropathogenic *E. coli* [24]. CNF1 enters the cell through clathrin-independent endocytosis. As the endosome matures and the pH drops, the toxin inserts into the membrane and translocates across the membrane of the late endosome and consequently releases the catalytic domain into the cytosol [25] [17]. Inside the cytosol, the catalytic domain acts on a GTPase, a member of the Ras protein family: RhoA [26, 20]. Deamidation of residue 63 in Rho, converting glutamine into glutamic acid, causes constitutive activity [8] [27]. Since RhoA is involved in actin polymerization, activation causes rearrangement of the actin cytoskeleton in the infected cell [28]. The deamidation seems to be catalyzed by a Cys-His catalytic diad at the active site [29] [30].

1.8 Cytotoxic Necrotizing Factor Y (CNFY)

Work on CNFY has only recently been expanding. There is still much that we do not know about the toxin. CNFY is a Type III toxin produced by *Yersinia pseudotuberculosis* [31]. In terms of amino acid sequence, it is 61% identical to that of CNF1. CNFY also takes the same route as CNF1 into the cytosol, following the endosomal pathway and translocating across the late endosome as the compartment acidifies [18]. There is also some overlap in binding receptors between CNF1 and CNFY [18]. Once in the cytosol CNFY selectively targets RhoA,

8

deamidating the Gln^{63}, similar to CNF1 [32]. The downstream effects result in multinucleation and formation of stress fibers [32].

1.9 Previous Inhibition Studies on PMT and CNF

Toxin translocation and trafficking properties were compared among members of the CNF family, CNF1, 2, 3, and Y, as well as to PMT [19], as described a previous study of PMT [16]. The reasoning behind this is comes from the N-terminal sequence similarity between PMT and CNF1, which may point to a functional similarity (Figure 1.3). Using SRE-luciferase as a reporter assay, the intracellular activities of PMT, CNF1, 2, 3, and Y were compared. Testing included inhibition with varying concentrations of BafA1, cytochalasin D, nocodazole, LY294002, NH$_4$Cl, and BFA. While the results were able to confirm the entry of PMT and CNF into the cytosol from the late endosome, there were also notable differences between the cellular response to PMT, CNFY, and CNF3 and that of CNF1 and CNF2. It has also been previously shown that protonation of specific residues in the translocation domain affect the translocation of the catalytic domain [25].

The findings indicated that CNF1 and CNF2 increased activity under low levels of inhibitor concentrations, specifically BafA1 and NH$_4$Cl, while CNFY and PMT did not. However, at higher levels of inhibitor concentrations, activity was reduced for both PMT and all CNFs studied. This caused speculation as to whether this phenomenon was due to the differences in net charge in the N-terminus, which is presumably responsible for translocation, or the difference in the pI of this same region. The difference in pI for CNF1 and CNF2 is over 2 units higher than that of CNF3, CNFY and PMT in the region of residues 119-267 of CNF1 (and corresponding regions of CNF2, 3, Y and PMT). CNF1 and CNF2 have a net charge of 2 in this region while CNF3 and Y have a net charge of -4 and -3 for PMT [19].

Figure 1.3
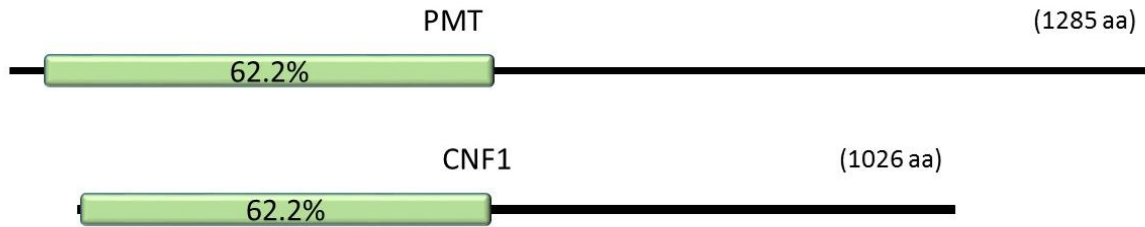
Protein Sequence Alignment Comparison of PMT and CNF1: Using FASTA for alignment, we find that PMT and CNF1 share high similarity on the N-terminus [37]. There is a 62.2% sequence similarity between residues 29-607 on PMT and residues 8-564 on CNF1. There is a 25.5% identity consensus on the compared sequence as well. These regions fall within the N-terminus of the proteins, which acts as binding and translocation function for toxin entry.

This being so, it is possible that chimeric CNFs with mutations in those specific translocation domain residues would also affect translocation. A practical way to test this would be to use different translocation domains from closely related CNF toxins while retaining the original activity domain. Due to knowledge of previous data on the activity of CNF1, 2, and Y, it follows to use these toxins as a basis for these experiments. Translocation regions in CNF1 and CNF2 are similar to each other but dissimilar to that of CNFY. Switching the translocation domain of CNFY with that from CNF1 and CNF2 allows us to determine if the translocation domain is responsible for the observed differences in activities and to possibly isolate differences to a specific region.

1.10 Construction of Chimeric Proteins

Hypothesis

To further explore this hypothesis, we generated a series of chimeric CNFs and performed comparative analyses on them as previously described [19, 16]. Using SRE-luciferase reporter assay as an indicator for activity, we wanted to test these chimeric proteins under varying concentrations of inhibitors to see if the increase in activity can be localized to a responsible domain.

In this study, I aim to start construction and isolation of the chimeric CNFs so that further testing can be done on them. We will make a chimeric protein by swapping the catalytic C-terminal of CNFY with that of other CNFs, while keeping the receptor binding and transmembrane domain constant (Figure 1.4). CNFY N-terminal with CNF1 C-terminal protein would be labeled CNFY1. Thus, the different constructs that I would be comparing are: CNFY, CNF1, and CNFY1. Running this chimera against the wild type CNFY and CNF1 under different levels of inhibitor, we will be able to determine a number of things. First, if CNF1 N-terminal is changed to CNFY, a change of activity may mean that the difference between CNF1 and CNFY activity is caused by translocation efficiency. This allows us to narrow down the differences in translocation activity to the N-terminal (and the role of residues 199-267 in the translocation process). Second, with CNFY C-terminal is changed to that of CNF1, we want to see if any change in activity for CNFY1 could be attributed to the catalytic domain.

Figure 1.4
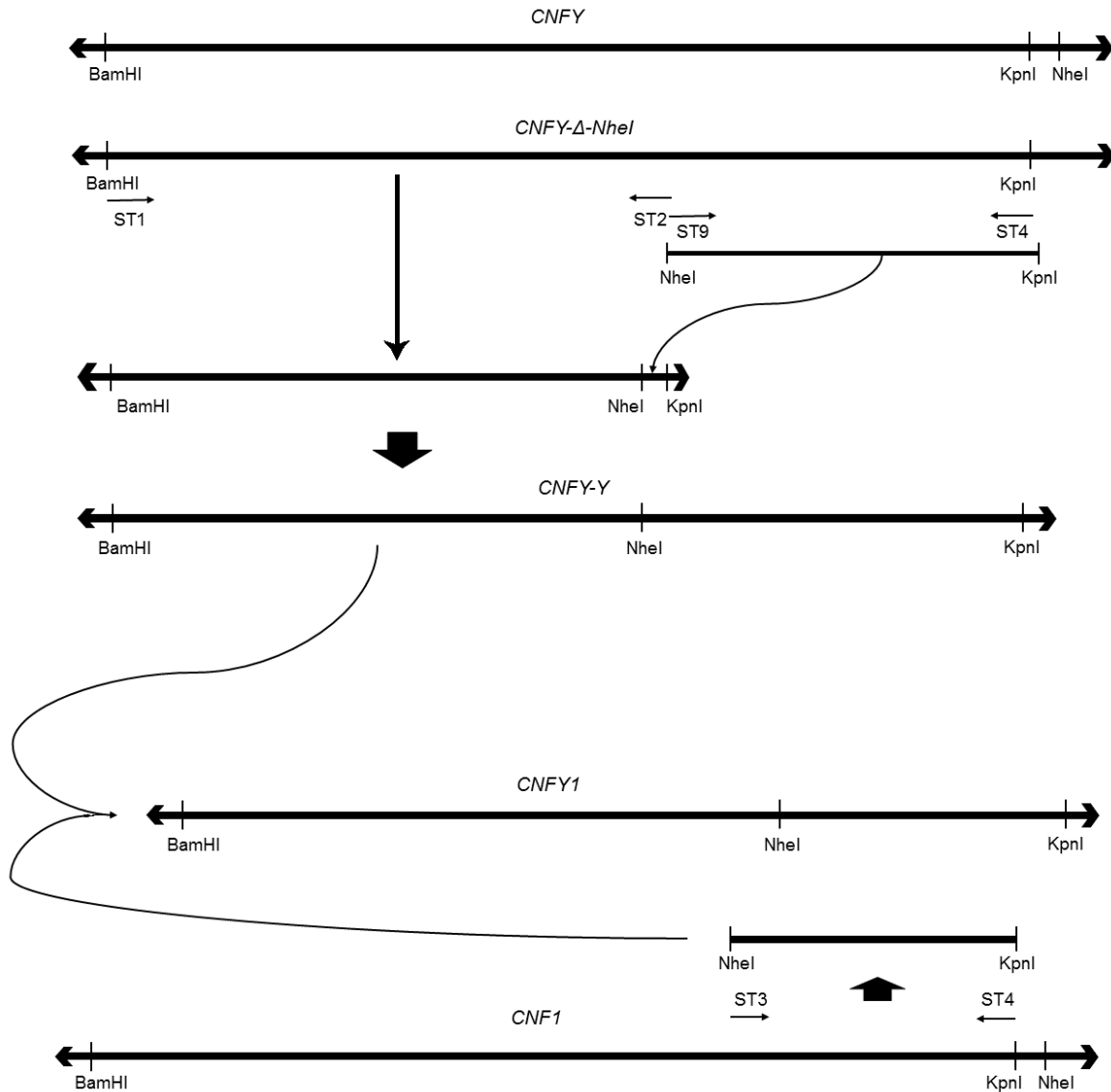
Construction of CNFY-Y and chimeric swap: CNFY gene in the original plasmid is taken and the NheI site is removed. This becomes the CNFY-ΔNheI construct. From this construct, a new 2 kbp fragment is created via PCR and reintroduced into the plasmid, making an intermediate construct that now contains BamHI, NheI, and KpnI. The C-terminus is created from CNFY-ΔNheI via PCR and ligated into the intermediate construct between NheI and KpnI to create CNFY-Y. CNFY-Y is used as a template for other chimeric constructs. To create CNFY1, the C-terminal PCR fragment from CNF1 replaces the fragment between NheI and KpnI on CNFY-Y.

Chapter 2: Methods

2.1 Bacterial Strains, Cloning, and Mutagenesis

Plasmid constructs

DNA for *cnf1*, and *cnfy* was generated via PCR from their original plasmids. pQE-CNF1 was obtained from Dr. Alison O'Brian at Uniformed Services University and pQE-CNFY was by Tana Repella of Wilson Lab from genomic DNA isolated from *Y. pseudotuberculosis* strain YPIII [19]. pQE-CNFY was first treated with NheI, blunt-ended with Mung bean nuclease and religated with T4-DNA ligase. This Δ-NheI-pQE-CNFY was then used for introduction of a new NheI site between N-terminal 2 kbp and c-terminal 1 kbp fragment to generate pQE-CNFY-Y (Mengfei Ho and Stephanie Tham)(Figure 1.3). With this new NheI site and the N-terminal BamHI site, C-terminal KpnI site, pQE-CNFY-Y was used to generate chimera CNFY1. A list of all the primers used is shown. (Table 2.1)

cnfy1

CNF1-C terminal was cloned out from a primer added NheI site to the KpnI site on the pQE-CNF1 plasmid. CNFY-N terminal was cloned out from the BamHI site to a primer added NheI site on pQE-CNFY. CNFY-N and CNF1-C are ligated together at the NheI site and ligated into the pQE vector from the BamHI site to the KpnI site resulting in the final vector (Figure 2.1).

superG-cnfy1

The *cnfy1* construct was PCR cloned from the BamHI to the KpnI site. Primer mutagenesis converted the N-terminal BamHI to a KpnI site and the C-terminal KpnI site to a NotI site. This fragment was ligated into the superG vector replacing the GFP gene. The superG vector is an engineered pGEpi-GFP vector for high expression of protein with a His tag, a thrombin-cleavage site and a KpnI site in front of GFP and a Not I site at it end (Mengfei Ho). The pGEpi vector was previously used and is itself a modified version of the pTrcHisC vector with a GFP tag added from the pGFPuv vector [33] (Figure 2.2). The construct was transformed into TOP10 cells for expression.
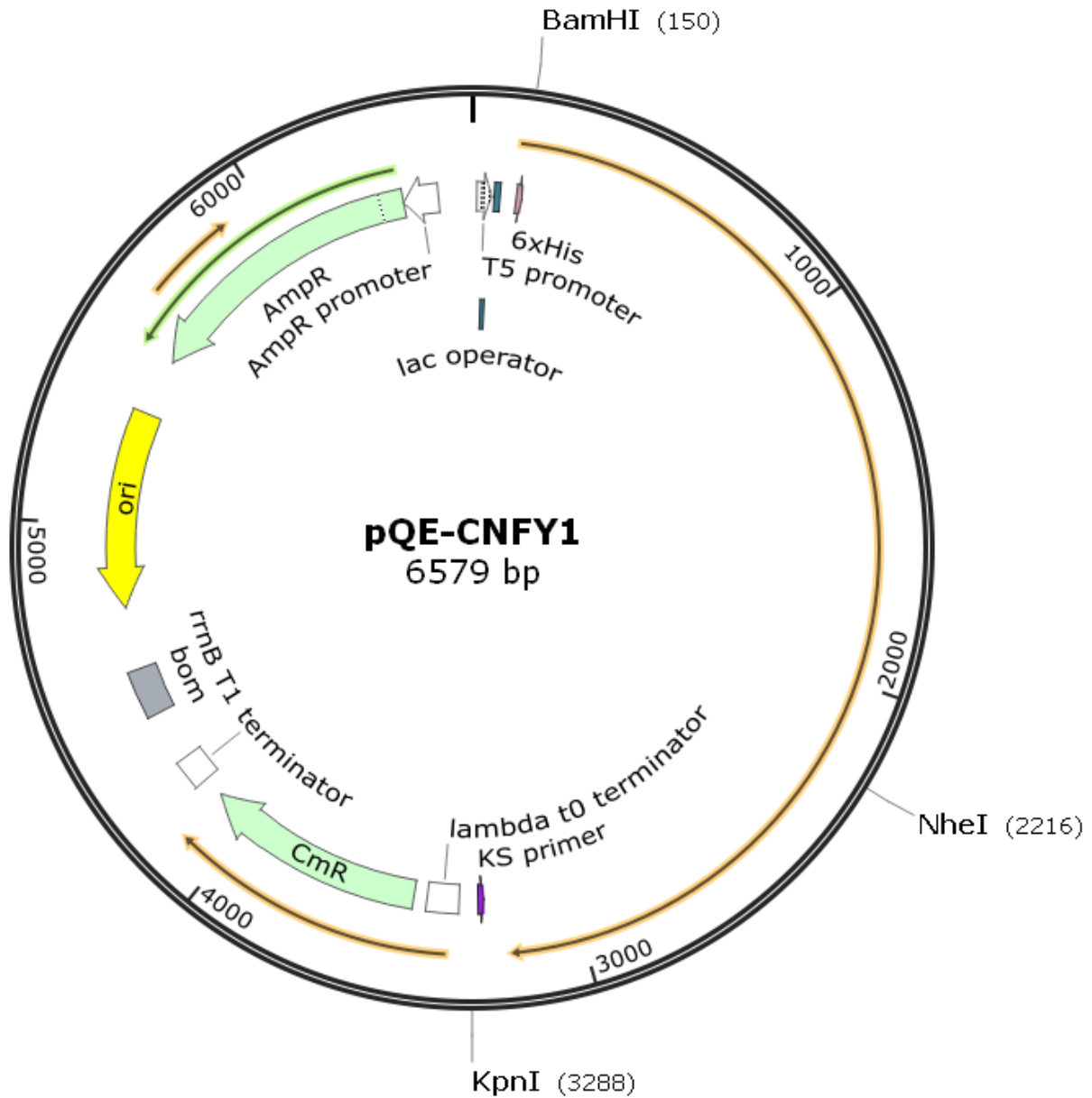
Table 2.1 Primer list:
PCR primers were used to generate PCR fragments of the different N and C-terminals from the plasmids.

ST1	TCACCATCACCATCACCATCACGGATCCATG
ST2	GAAGAGGTACCGTCTGTCCACAACTGCTAGCACTTCTACAGGTGCTTCATC
ST3	GATGAAGCACCTGTAGAAGTGCTAGCAGTTGTGGACAGACGGTTT
ST4	GACCCGGGGTACCACGGC
ST9	GTAGAAGTGCTAGCAGTTGTGGACAG

Figure 2.1
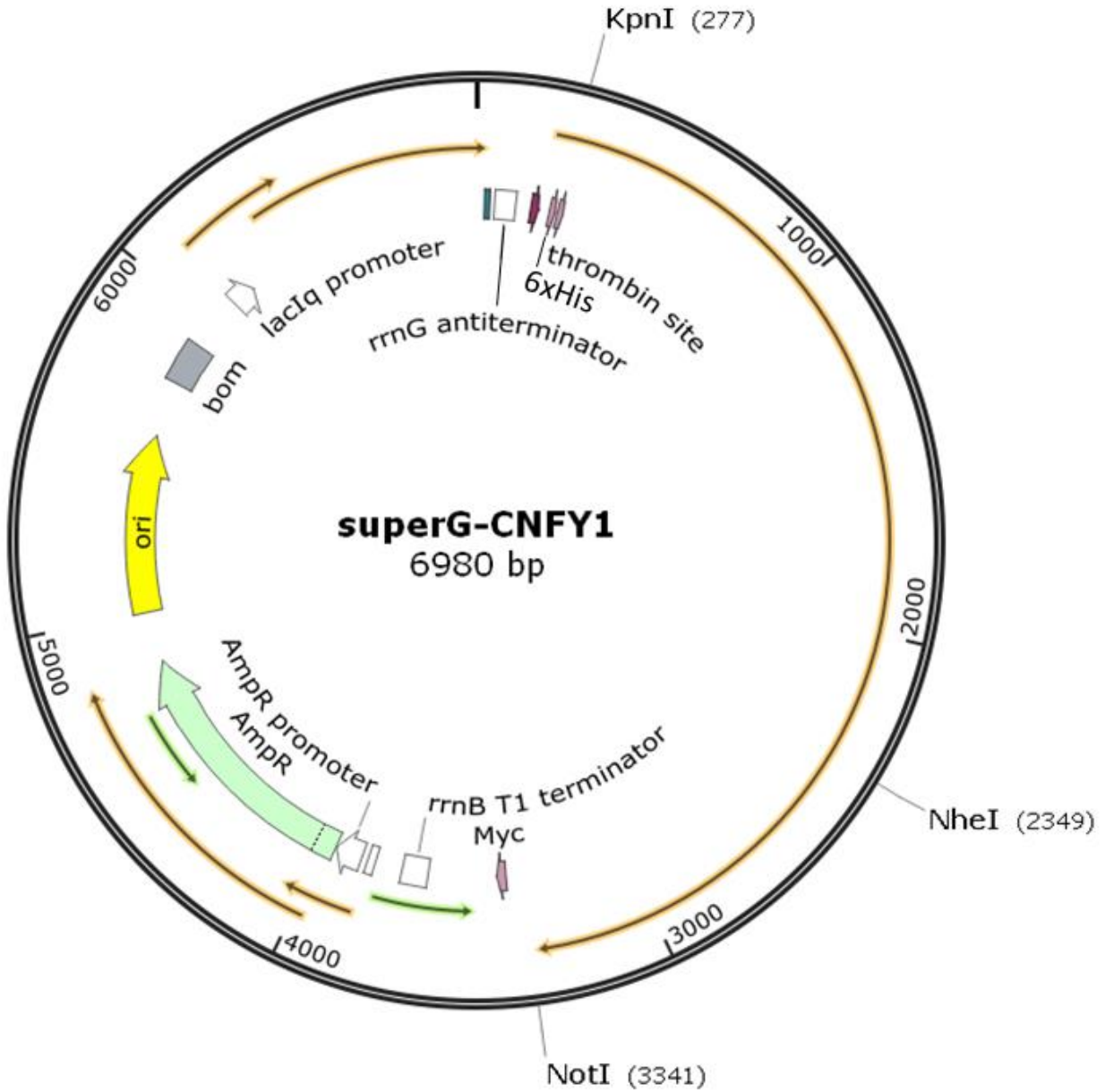

CNFY1 in pQE vector plasmid map: The CNFY1 plasmid is a chimeric DNA construct from pQE-CNFY, pQE-CNF1, and pQE-CNFY-Y. There is a PCR introduced NheI site between the catalytic domain and the binding and translocation domain. This construct was used to produce to produce the superG-CNFY1 plasmid as well as the CNFY1 protein.

Figure 2.2

CNFY1 in superG vector plasmid map: The CNFY1 insertion PCR modified to start with KpnI replacing BamHI and ending with NotI replacing KpnI. This new insert was ligated into the superG vector. This vector was then transformed into TOP10 cells for expression.

DNA Amplification

All DNA constructs in their respective vectors were then transformed into *Escherichia coli* TOP10 cell cultures. TOP10 cells were prepared using the Inoue method for competent cells [34]. Cells were grown in LB medium overnight at 37 °C and stored in 25% glycerol at -80 °C.

2.2 Protein Expression

CNFY1

Starting from glycerol stock cultures, a Luria agar plate with 100 ug/mL ampicillin was streaked. The plates were grown overnight at 37 °C and single colonies are picked and used to inoculate 5 mL Luria broth tubes with 100 ug/mL ampicillin. Tubes were grown overnight at 37 °C. 1 mL of each tube culture was taken and put into flasks 500 mL Luria broth with 100 ug/mL ampicillin, 8 flasks in total. Flasks were incubated at 37 °C until optical density of 0.8-1.0 at the 600 nm wavelength. The flasks were induced with 10 ug/mL of isopropyl-beta-D-thiogalactopyranoside (IPTG). Flasks were then incubated at room temperature (25 °C) overnight. Cells were harvested and spun down at 6000 rpm at 4 °C. Supernatant was discarded and the cells were resuspended in 200 mL Lysis buffer (1x PBS, a few drops of Igepal CA-630, 200 mg benzamidine, 60 mg lysozyme, 60 mg PMSF, protease inhibitor (Sigma-Aldrich P8849), DNase (Sigma-Aldrich D5025), and RNase (Sigma-Aldrich R6513)) and sonicated to lyse contents. The suspension was centrifuged at 13,500 rpm for 2 hours at 4 °C. The supernatant was taken and run through a HIS-Select® HF Nickel Affinity Gel (Sigma-Aldrich) under pH 7.5 Tris buffer and eluted into a HiTrap Q HP column (GE Life Sciences) under pH 7.5 Tris buffer with 100 mM imidazole. The column, with the protein bound, was then equilibrated with Tris buffer to pH 6.5 and eluted out with a increasing salt gradient of 1 M sodium chloride in pH 6.5 Tris buffer with 10 mL fractions caught at 0.1, 0.2, 0.22, 0.25, 0.3, 0.33, 0.35, 0.37, 0.50, and 1 M. 5 µL of each fraction was run on an 8% SDS-PAGE gel. Gels were stained with Coomassie Blue for visualization (Figure 3.4).

superG-CNFY1

Procedures are similar to CNFY1 purification except the 1M NaCl gradient used was 0.1, 0.2, 0.25, 0.33, 0.35, 0.4, 0.5, and 1 M. 5 µL of each fraction was run on an 8% SDS-PAGE gel. Gels were stained with Coomassie Blue for visualization (Figure 3.5).

CNFY

      Cell culture is from unmodified CNFY in pQE plasmid. Procedures are similar to CNFY1 purification except the 1 M NaCl gradient used was 0.1, 0.2, 0.2, 0.2, 0.22, 0.25, 0.3, 0.35, 0.5, and 1 M. 5 µL of each fraction was run on an 8% SDS-PAGE gel. Gels were stained with Coomassie Blue for visualization (Figure 3.1, 3.2).

CNF1

      Cell culture is from unmodified CNF1 in pQE plasmid grown in XL1-Blue cells. Protein expression in XL1-Blue showed stronger expression than in TOP10. Procedures are similar to CNFY1 purification except the 1 M NaCl gradient used was 0.1, 0.15, 0.2, 0.2, 0.22, 0.25, 0.3, 0.5, and 1.0 M. Samples (5 µL) of each fraction were run on an 8% SDS-PAGE gel. Gels were stained with Coomassie Blue for visualization (Figure 3.3).

2.3 Protein Concentration

      Relevant fractions of the eluted protein were loaded onto a HIS-Select® HF Nickel Affinity Gel column at pH 7.5 and eluted into a HiTrap Q HP column with 100 mM imidazole at pH 7.5. The column was equilibrated with Tris buffer to pH 6.5 and the protein was eluted out with a 1 M NaCl in Tris buffer gradient at pH 6.5 in 1 mL fractions. The gradient increases 0.1 M each step with 2 fractions collected at each step and finishing with 6 fractions of 1 M NaCl. A Bradford assay was done to determine fractions containing the target protein. Samples (1 µL) of relevant fractions were then run on an 8% SDS-PAGE gel and stained with Coomassie Blue for visualization (Figure 3.6-3.9). All proteins were then desalted using PD-10 Desalting Column (GE Healthcare) in phosphate buffered saline (PBS) with 10% glycerol and collected into 0.5 mL fractions. Proteins are stored at -80 ºC in PBS with 10% glycerol.

Chapter 3: Results

3.1 Purification of CNFY, CNF1, and CNFY1

  CNFY, CNF1, CNFY1, and superG-CNFY were successfully purified under the stated conditions (see Methods). Samples run on SDS-PAGE showed interesting results. There were consistently two major products resulting from the purification: a shorter version of CNFY1 and CNFY at around 100 kDa and a full-length version of each at the expected size of ~115 kDa. The smaller 100 kDa fragment also exhibited a yellow color, when eluting from the nickel agarose column. This fragment might have resulted from some form of nickel-chelation during the metal ion-chelation column chromatography step. This form eluted from the Q HP anion exchange column between 0.3 M and 0.35 M NaCl (Figure3.1). However, the expected protein length is 114 kDa to 116 kDa for a full-length CNF protein. In the longer versions purified, the protein eluted at 0.2 M NaCl and is about 115 kDa in size (Figures 3.1-3.5).

  The proteins were concentrated from the purified samples containing relevant protein with a HiTrap Q HP column (See Methods). Some purification samples were combined with previous samples to give higher density protein after concentration. The long version of CNFY and superG-CNFY1 were concentrated from just one purified preparation. The short version of CNFY and CNF1 were concentrated from two previous preparations respectively. The shorter version of CNFY1 was not concentrated. (Figures 3.6-3.9)

Figure 3.1
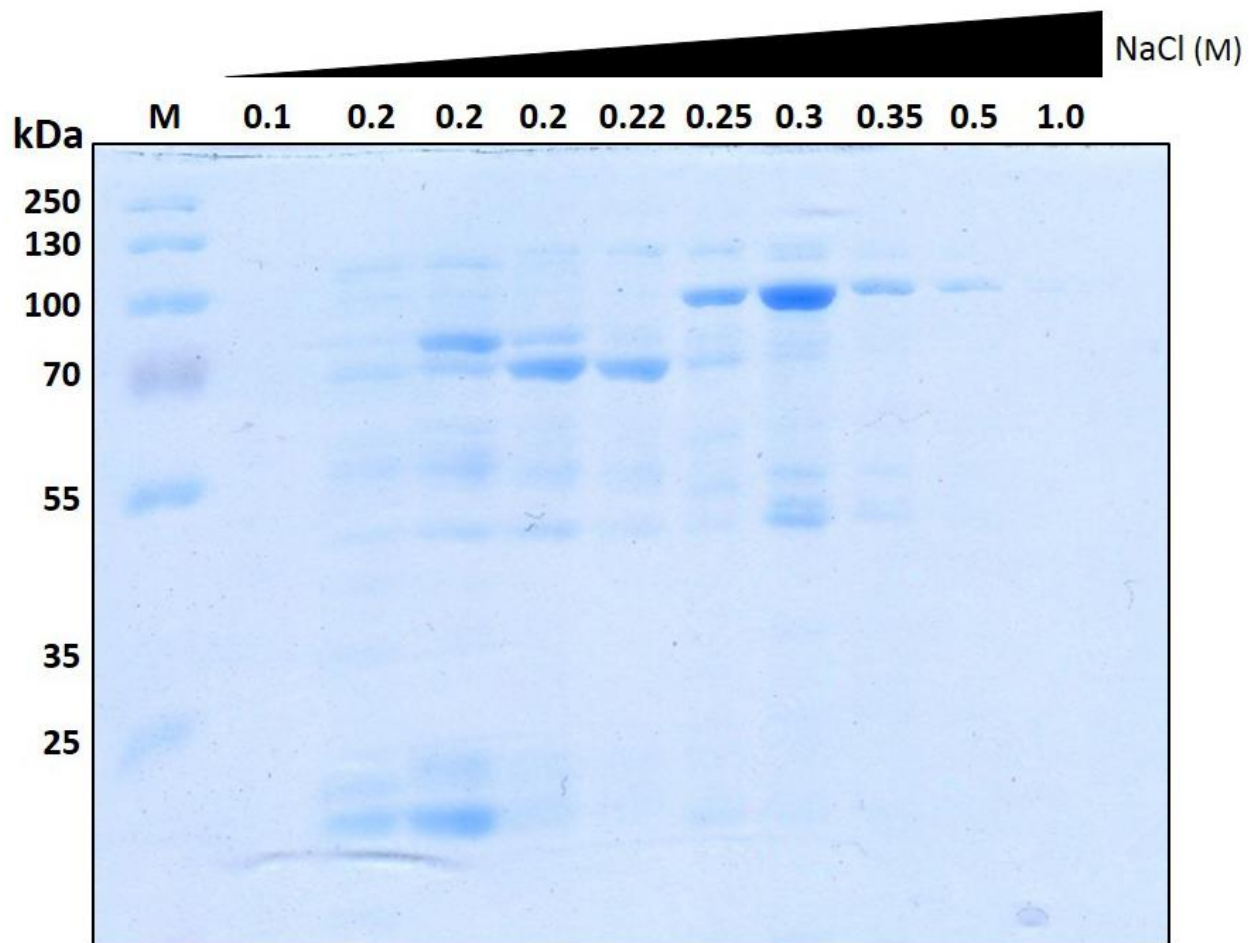
Purification of CNFY short version: The short version of CNFY eluted out from a Q HP ion exchange column at 0.25 M to 0.35 M of NaCl. The size was around 100 kDa which is smaller than the expected 115.8 kDa size. Out of each 10 mL fraction of eluent collected, an equivalent of 2 μL was loaded into each well. This gel was run on 10% SDS-PAGE. The 0.25 M to 0.5 M fractions were taken for concentration.
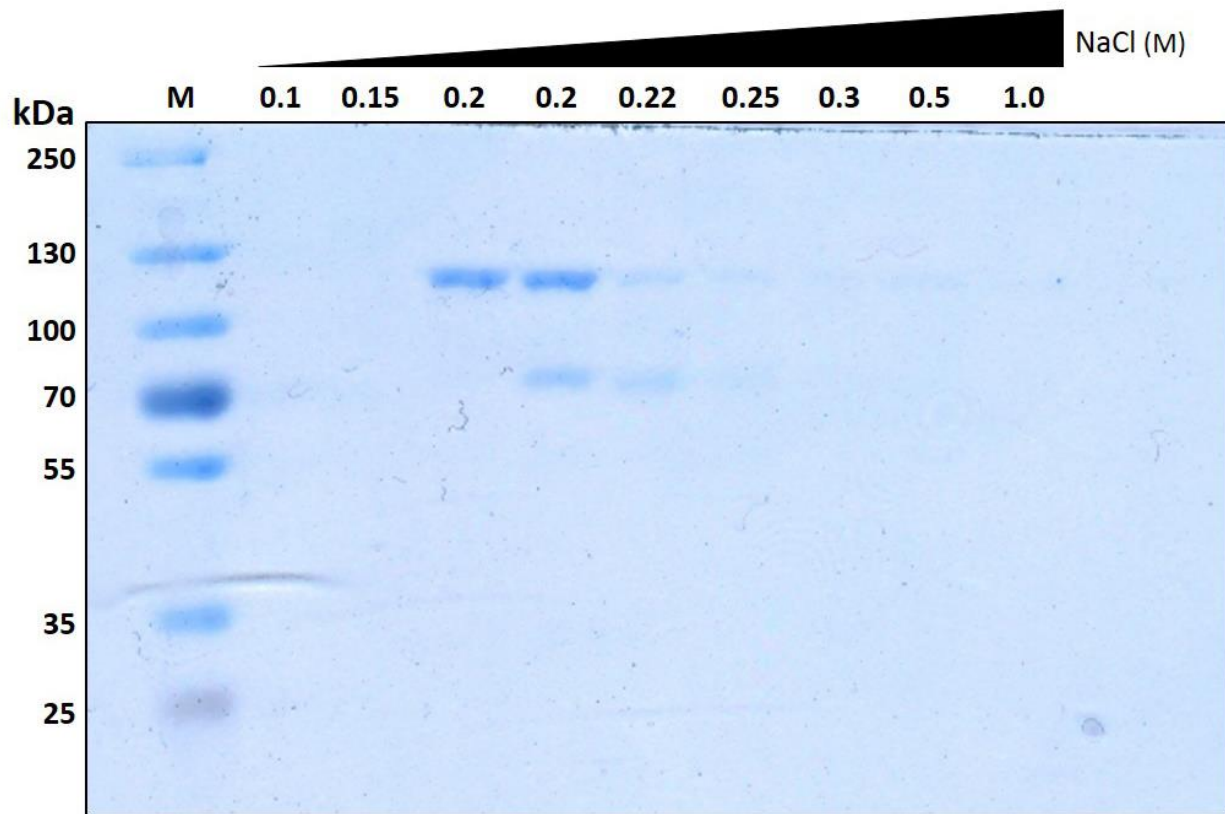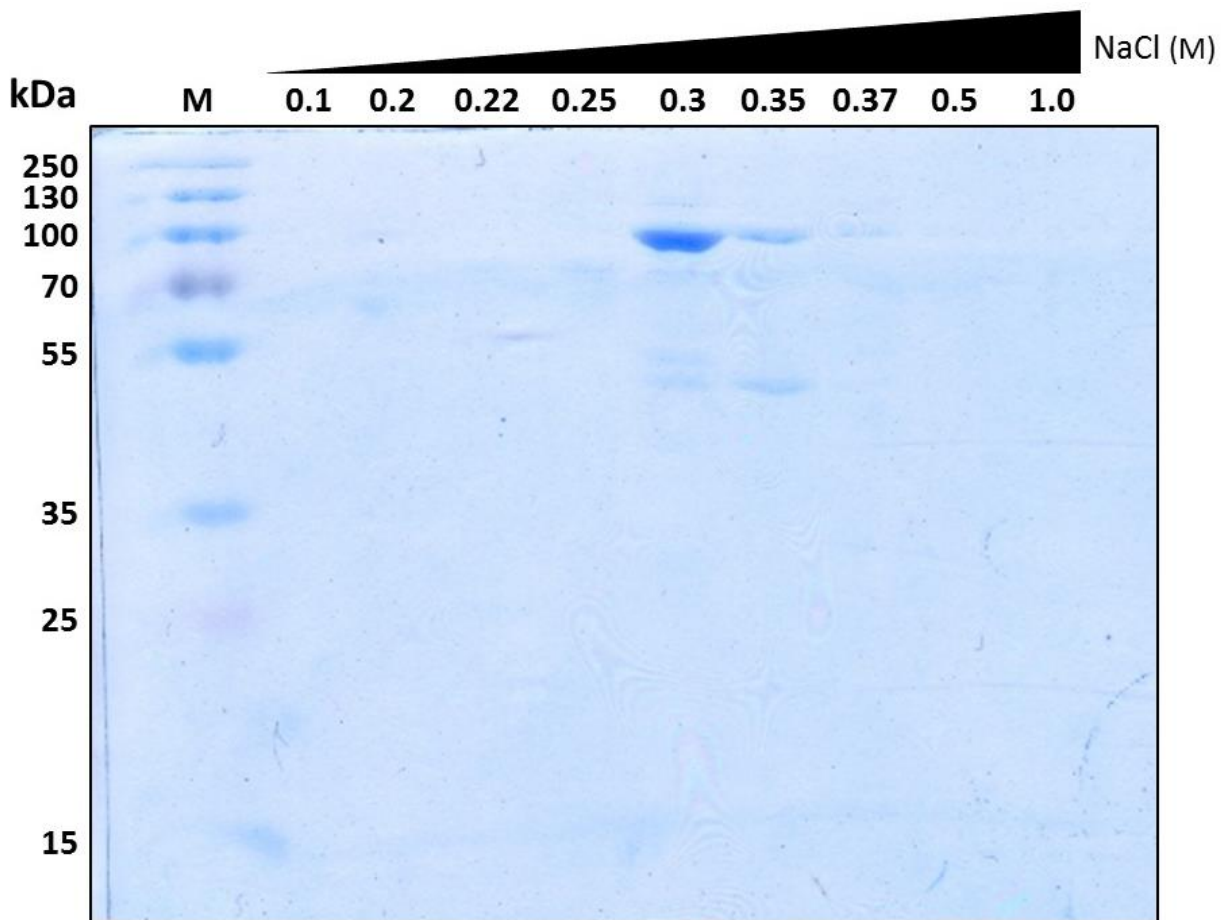
Figure 3.2
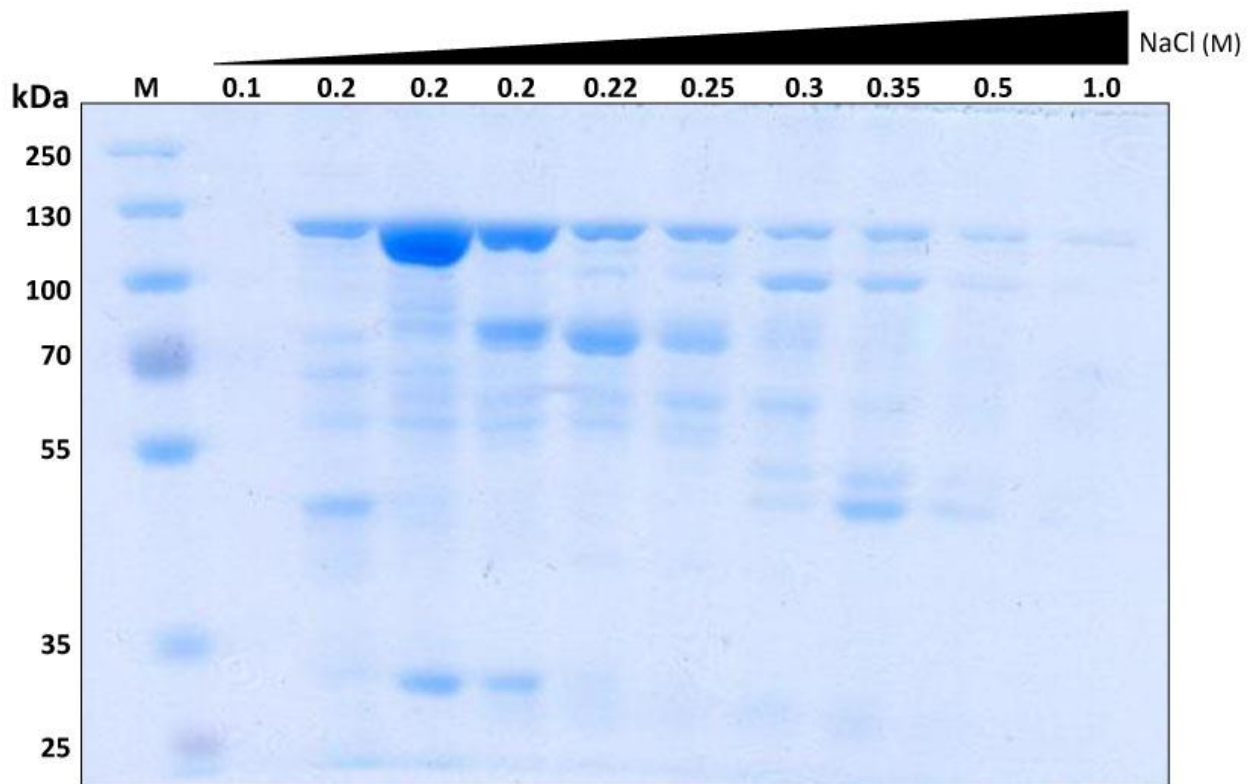
Purification of CNFY long version: The long version of CNFY is eluted out from a Q HP ion exchange column between 0.2 M and 0.25 M NaCl. The size is around the expected 115.8 kDa. Out of each 10 mL fraction an equivalent of 2 μL was loaded into each well. This was run on an 8% SDS-PAGE gel. The first two 0.2 M fractions were taken for concentration.

Figure 3.3

Purification of CNF1: CNF1 was eluted out from a Q HP ion exchange column at 0.2 M NaCl. The size is around the expected 115.2 kDa. Out of each 10 mL fraction an equivalent of 2 μL was loaded into each well. This was run on an 8% SDS-PAGE. The two 0.2 M fractions were taken for concentration.

Figure 3.4

Purification of CNFY1 short version: The short version of CNFY1 eluted out from a Q HP ion exchange column between 0.3 M and 0.35 M NaCl. This protein is around 100 kDa, which is shorter than the expected 116.2 kDa. Out of each 10 mL fraction, an equivalent of 2 µL was loaded into each well. This was run on a 10% SDS-PAGE gel.

Figure 3.5
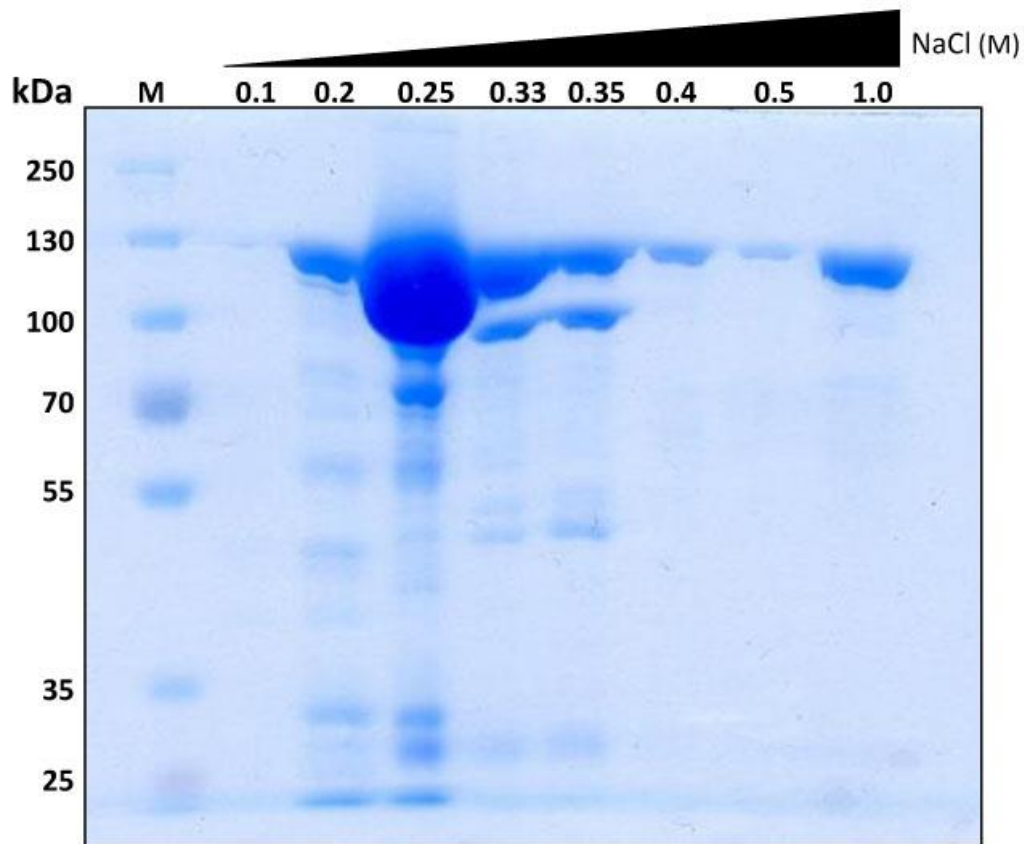
Purification of CNFY1 long version: superG-CNFY1 yielded the long version of the CNFY1 protein and eluted out from a Q HP ion exchange column between 0.2 M and 0.35 M NaCl. The extension into the later fractions was probably caused by the large quantity of proteins to elute out. The proteins are around the expected 116.2 kDa. An equivalent of 2 μL from each 10 mL fraction was loaded into each well. This was run on an 8% SDS-PAGE gel. The 0.2 M and 0.25 M fractions were taken for concentration.

Figure 3.6
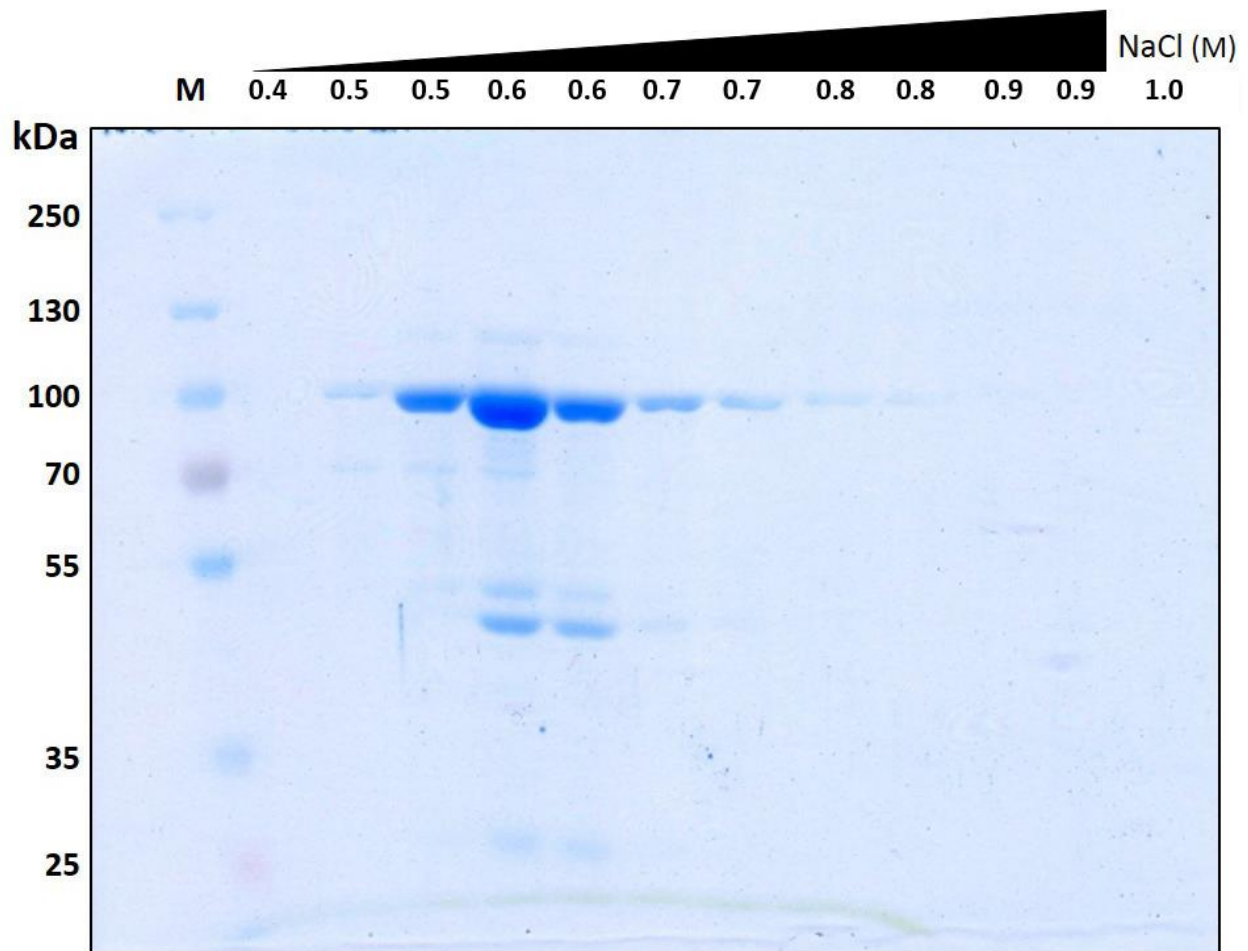
Concentration of CNFY short version: The short version of CNFY is concentrated down into 1 mL fractions using an increasing NaCl gradient on a Q HP ion exchange column. An equivalent of 1 μL from each fraction is loaded into each well. This is run on an 8% SDS-PAGE gel and once again confirms the 100 kDa size.

Figure 3.7
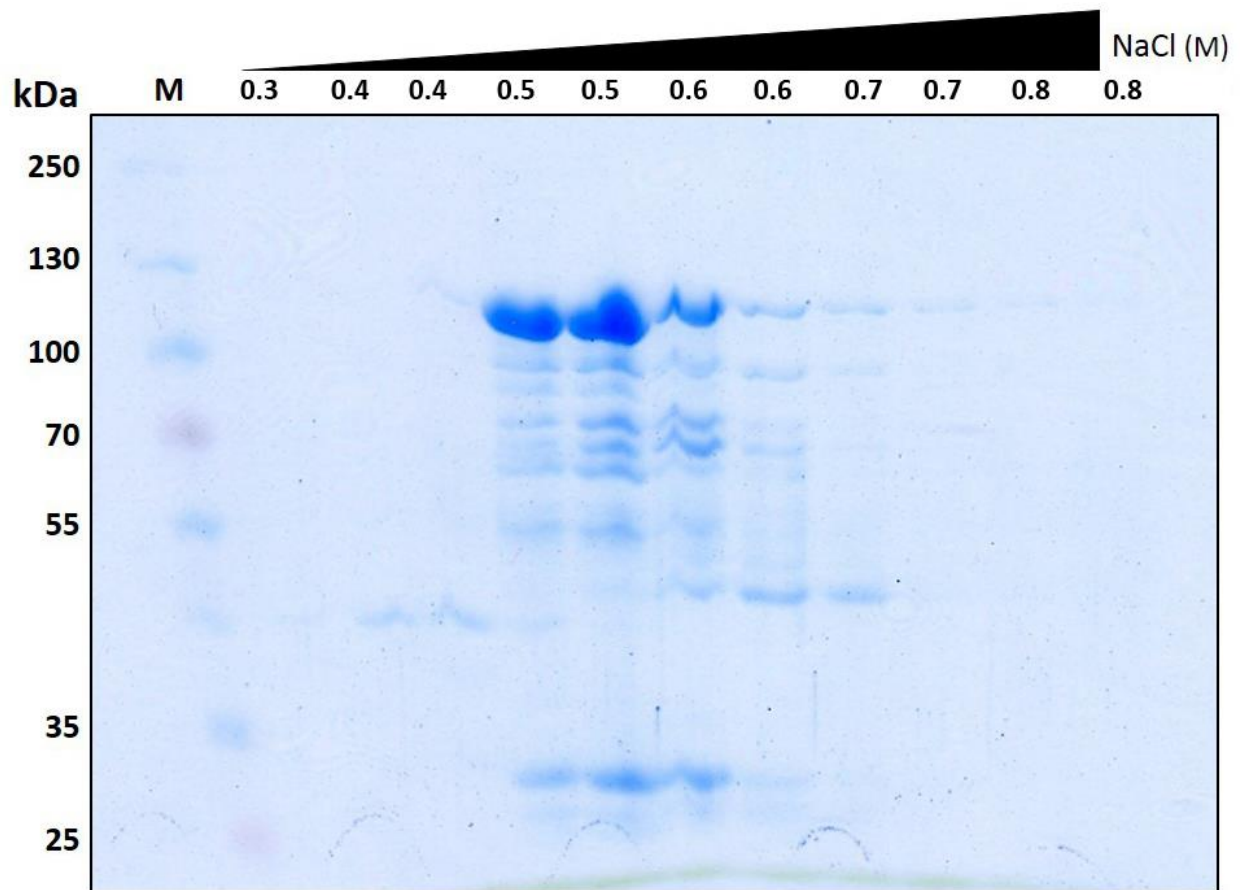
Concentration of CNFY long version: The long version of CNFY is concentrated into 1 mL fractions using an increasing NaCl gradient on a Q HP ion exchange column. An equivalent of 1 μL from each fraction is loaded into each well. This was run on an 8% SDS-PAGE gel.

Figure 3.8

Concentration of CNF1: CNF1 is concentrated down into 1 mL fractions using an increasing NaCl gradient on a Q HP ion exchange column. An equivalent of 1 µL from each fraction is loaded into each well. This is run on an 8% SDS-PAGE gel.
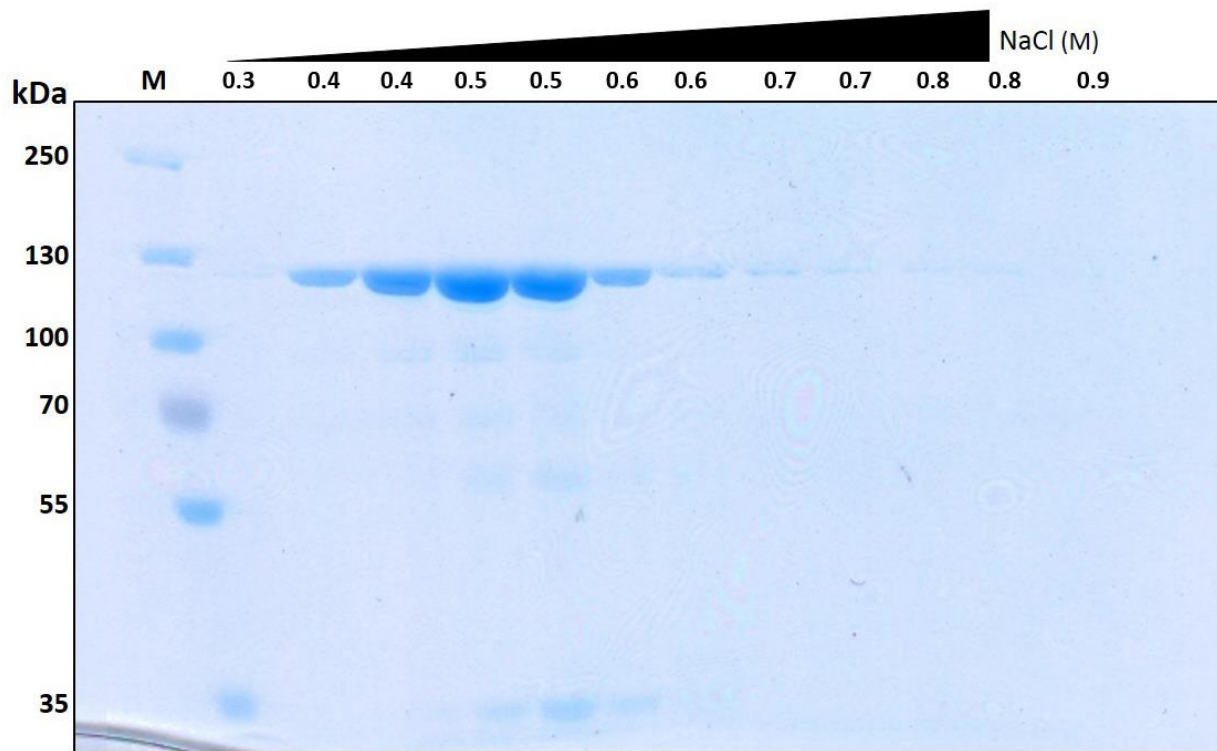
Figure 3.9

Concentration of CNFY1 long version: superG-CNFY1 was concentrated down into 1 mL fractions using an increasing NaCl gradient on a Q HP ion exchange column. An equivalent of 2 μL from each fraction was loaded into each well. This was run on an 8% SDS-PAGE gel.
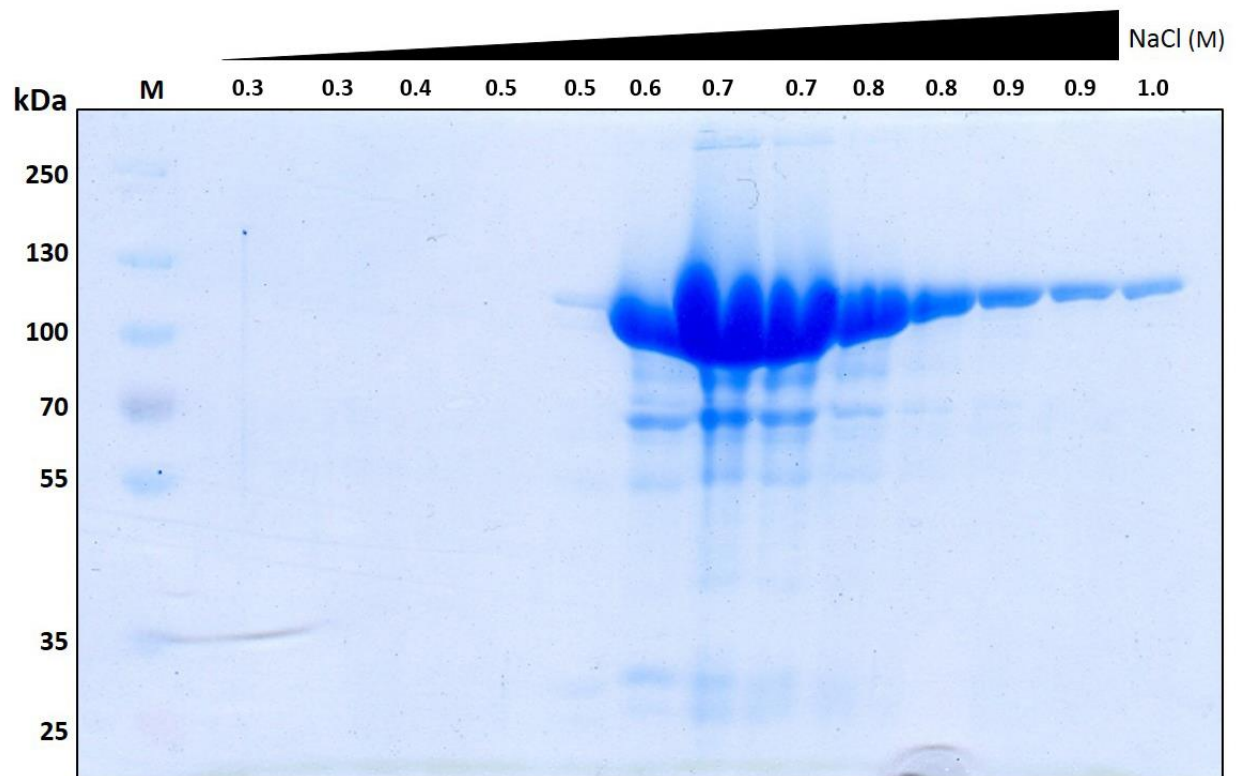
Chapter 4: Discussion

4.1 Production Efficiencies

During protein production, there appeared two different variables that contributed to production efficiency. In TOP10 cells, protein production was significantly diminished. CNF1 was optimally purified from XL1-Blue cells. This is in agreement with previous studies showing that CNF1 and CNF2 produced well in XL1-Blue cells [19]. The identity of the expression vector also has profound effects on the efficiency of protein production. The engineered superG vector seems to have amplified production many times over the original pQE vector. In comparing the short version of CNFY1 from a pQE vector and the long version from the superG vector, there is a dramatic difference in production (five-fold estimate). The superG vector has been engineered to have protein production capabilities without need for induction [33]. Current studies are to move all constructs into superG vectors for two reasons: to increase volume of protein production and to reduce degradation of product that was seen in CNFY1 protein purification. It is possible that this vector could be effective for other protein constructs as well.

4.2 Differential Fragments

During cultivation and purification of proteins, there were two distinct sizes of proteins that were eluted out. For both CNFY1 and CNFY, two consistent products were seen at a size of about 100 kDa and at the expected size of about 115 kDa. Each of the products was consistent in elution activity at certain pH as well. The larger 115 kDa product consistently eluted in earlier fractions than the smaller 100 kDa product. Consistent appearance indicates that the fragment is probable to have been generated during protein production in the bacteria. It is likely that the smaller fragment is derived from the larger one due to the fact that they both appear together during protein purification: one as a major product and one as a minor product. Both also have a His-tag so it is likely that amino acids lost from the C-terminal of the longer version produce the more acidic shorter version. During elution from a HiTrap Q HP column using a salt gradient, higher charged proteins, more acidic in this column, elute out later.

If we look at the CNFY1 protein sequence, it is 116 kDa, 1027 residues, and has a pI of 5.11. If the C-terminus of the protein is cleaved to 98.6 kDa and 866 residues, the pI becomes 5.04. If the entire C-terminus is cleaved, the pI becomes 4.84, but the size is reduced to 80 kDa and 704 residues. However, a shorter CNFY does not produce a significant change in the pI of the protein unless the entire C-terminus is cleaved (Table 4.1). The experimental data showed that the shorter fragment is more acidic as it elutes out at higher salt concentrations. We would need to see a decrease in protein pI in conjunction with the loss of amino acids to support this.

One other way to test for the unknown fragment would be to run both fragments on an SRE-luciferase assay and assess activity. The prediction is that the shorter fragment should show little to no activity if it is missing the C-terminal catalytic domain. A CNF toxin missing the activity domain would be useful as a control for the activity domain.

4.3 Other Constructs

With CNFY1 created, it is now possible to generate other constructs. Expanding beyond CNFY and CNF1, we can also look at CNF2. The pI of CNF1 differs from that of CNFY within the 119-267 equivalent region on CNF1 by over 3 pH units (7.65 and 4.67 respectively). However, a few residues are not conserved between CNF1 and CNF2 (Figure 4.1). In contrast, CNF1 and CNF2 differ in this critical region by about 0.3 pH units (7.65 and 7.91 respectively). Elucidating the repercussions of this difference could help us narrow down the responsible residues for the differential behavior among CNF1, CNF2 and CNFY. Creating other chimera constructs would give us more information in this direction. This being so, we have started work on constructing chimeric proteins between CNF1 and Y, and CNF2 and Y, switching both the N-terminal and C-terminal domains (Figure 4.2).

Table 4.1 Comparison of pI values within the N-terminal domains of CNFY1 and CNFY:
CNFY1 shows a steady decrease in pI as C-terminal residues are removed, this supports the data indicating that the 100 kDa product is the shorter, more acidic version of the longer one. CNFY does not show this trend until the entire C-terminal domain is cleaved, at which point, the amino acid sequence is identical with that of CNFY1.

CNFY1			CNFY		
Residues	pI	Weight (kDa)	Residues	pI	Weight (kDa)
1027	5.11	116	1026	5.02	115
956	5.06	108	956	5.00	107
885	5.09	100	910	5.14	102
866	5.04	98.6	884	5.13	100
844	5.02	96.3	865	5.07	98.3
832	4.98	94.9	785	5.09	89.5
786	5.02	89.6	758	5.07	86.4
753	4.98	85.8	754	5.03	85.9
743	4.95	84.7	752	5.00	85.7
738	4.92	84.1	741	4.94	8.45
704	4.84	80.1	716	4.90	81.6
			704	4.84	80.1

Figure 4.1

```
CNFY   113 STAGIYKTNNADSFDETNEAKMLPSEYLYFLRDCDFSNLYNKALSDYWAENYEKFSTLLQ  172
CNF1   113 SSTGIYKTKSADVFNEENEEKMLPSEYLHFLQKCDFAGVYGKTLSDYWSKYYDKFKLLLK  172
CNF2   125 ASAGIYKTSSADMFNEKNEEKMLPSEYLYFLKGCDFSGIYGRFLSDYWSKYYDKFKLLLK  184
           :::*****..** *:* ** **********:**: ***: :* : *****:: *:**. **:


CNFY       NYYISSAYYLYKDSAISKDEYEFSIDAIFNKKSKILRYYFDVYGYYSSDMFVAMNDNKTM  230
CNF1       NYYISSALYLYKNGELDEREYNFSMNAL-NRSDNISLLFFDIYGYYASDIFVAKNNDKVM  231
CNF2       NYYISSALYLYKNGEIDEYEYNFSISAL-NRRDNISLFFFDIYGYYSSDMFVAKNNERVM  243
           ******* ****:. :.: **:**:.*: *: .:*   :**:****:**:*** *:::.*


CNFY       LFIPGATNPFIFADNITDLRDKIKALISDKNTRE  266
CNF1       LFIPGAKKPFLFKKNIADLRLTLKELIKDSDKQQ  265
CNF2       LFIPGAKKPFLFEKNIADLRISLKNLIKENDNKQ  277
           ******.:**:* .**:*** .:* **.:.:.::
```

Sequence alignment comparison of CNF1, CNF2, and CNFY: CNFY, CNF1, and CNF2 are compared on their residues from the 119-267 amino acid residues on CNF1 and corresponding residues on CNF2 and CNFY. ClustalW was used to align sequences [35] [36]. An asterisk (*) denotes a single, fully conserved residue, a colon (:) denotes a residue with strongly conserved properties, a period (.) denotes a residue with weakly conserved properties, and a blank ( ) denotes no conservation. Red denotes a small, hydrophobic, or aromatic residue (AVFPMILW), blue denotes an acidic residue (DE), magenta denotes a basic residue (RK), and green denotes a residue with a hydroxyl, sulfhydryl, or amine group (STYGCNGQ).

32

Figure 4.2
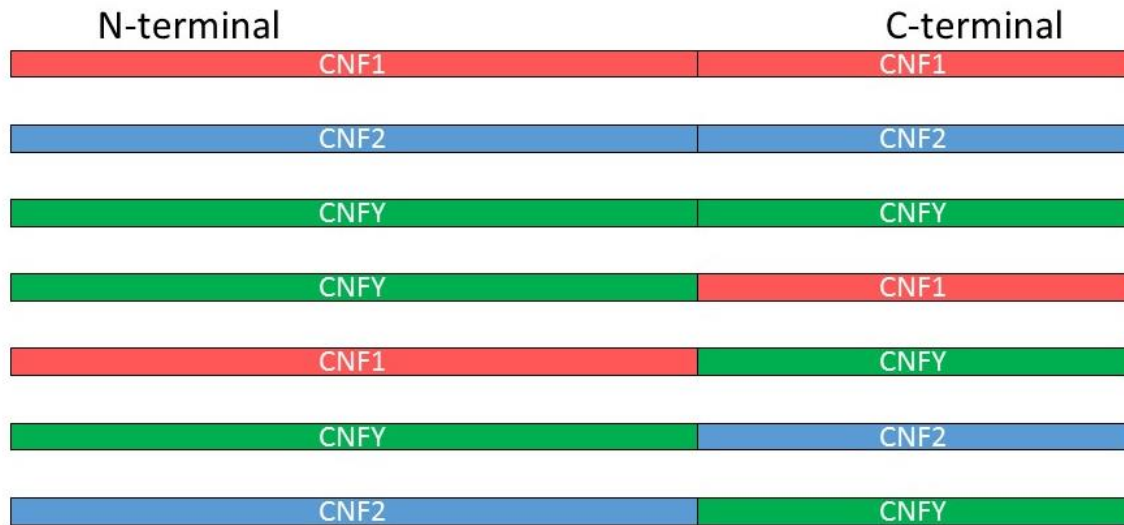
Possible CNF chimeric constructs: All the chimera constructs of interest are listed here, including the ones created in this thesis. Congruent N and C-terminal constructs signify the wild-type version of the toxin. By exchanging both N and C-terminals we will be able to run detailed analysis on the effects of each domain in regards to SRE-luciferase activity.

4.4 Future Direction

This project has developed a reliable method of generating and purifying CNF toxins and chimeric constructs thereof. Our focus now is to finish construction of the possible chimeric permutations using CNF1, CNF2, and CNFY. Combining the N-terminal of CNF1 with the C-terminal of CNFY is the immediate goal, as it will provide an additional piece of information regarding the differences between CNF1 and CNFY. Due to CNF2 being more similar to CNF1 in residue sequence than CNFY, permutations of CNFY using CNF2 N and C-terminus is also being studied. Upon completion of these constructs, we will be able to test the chimeras using SRE-luciferase assays. We expect to see increased levels of activity in SRE-luciferase assays under low levels of inhibitor applied to the CNFY1 construct as compared to CNFY wild-type protein. Variable levels of inhibitors in the assay will allow us to reproduce the results described in the previous study [19], and to explore the functionality of chimeric constructs.

References

[1] F. M. Foss, "DAB389IL-2 (ONTAK): A Novel Fusion Toxin Therapy for Lymphoma," *Clinical Lymphoma,* vol. 1, pp. 110-116, 2000.

[2] M. Alami, M.-P. Taupiac, H. Reggio, A. Bienvenue and B. Beaumelle, "Involvement of ATP-dependent Pseudomonas Exotoxin Translocation from a Late Recycling Compartment in Lymphocyte Intoxication Procedure," *Molecular Biology of the Cell,* vol. 9, p. 387–402, 1998.

[3] Q. Yan, X.-P. Li and N. E. Tumer, "N-glycosylation Does Not Affect the Catalytic Activity of Ricin A Chain but Stimulates Cytotoxicity by Promoting Its Transport Out of the Endoplasmic Reticulum," *Traffic,* vol. 13, pp. 1508-1521, 2012.

[4] B. K. Kobilka and R. J. Lefkowitz, "STUDIES OF G-PROTEIN–COUPLED RECEPTORS," *Scientific Background on the Nobel Prize in Chemistry 2012,* pp. 1-15, 2012.

[5] M. Louet, L. Charlier, J. Martinez and N. Floquet, "Dissociation of membrane-anchored heterotrimeric G-protein induced by G(α) subunit binding to GTP," *Journal of chemical information and modeling,* pp. 3022-3027, 2012.

[6] J. Cherfils and M. Zeghouf, "Regulation of Small GTPases by GEFs, GAPs, GDIs," *Physiological Reviews,* pp. 269-309, 2013.

[7] M. S. Marshall, "Ras target proteins in eukaryotic cells," *The FASEB Journal,* pp. 1311-1318, 1995.

[8] G. Flatau, L. Landraud, P. Boquet, M. Bruzzone and P. Munro, "Deamidation of RhoA Glutamine 63 by the Escherichia coli CNF1 Toxin Requires a Short Sequence of the GTPase Switch 2 Domain," *Biochemical and Biophysical Research Communications,* p. 588–592, 2000.

[9] E. Oswald, M. Sugai, A. Labigne, H. C. Wu, C. Fiorentini, P. Boquet and A. D. O'Brien, "Cytotoxic necrotizing factor type 2 produced by virulent Escherichia coli modifies the small GTP-binding proteins Rho involved in assembly of actin stress fibers," *Microbiology,* pp. 3814-3818, 1994.

[10] M. Brothers, M. Ho, R. Maharjan, N. Clemon, Y. Bannai, M. Waites, M. Faulkner, T. Kuhlenschmidt, M. Kuhlenschmidt, S. Blanke, C. Rienstra and B. Wilson, "Membrane interaction of Pasteurella multocida toxin involves sphingomyelin," *The FEBS Journal,* vol. 278, p. 4633–4648, 2011.

[11] B. A. McNichol, S. B. Rasmussen, H. M. Carvalho, K. C. Meysick and A. D. O'Brien, "Two Domains of Cytotoxic Necrotizing Factor Type 1 Bind the Cellular Receptor, Laminin Receptor Precursor Protein," *Infection and Immunity,* vol. 75, no. 11, p. 5095–5104, 2007.

[12] J. M. Lord and L. M. Roberts, "Toxin Entry: Retrograde Transport through the Secretory Pathway," *The Journal of Cell Biology,* vol. 140, p. 733–736, 1998.

[13] J. R. Murphy, "Mechanism of Diphtheria Toxin Catalytic Domain Delivery to the Eukaryotic Cell Cytosol and the Cellular Factors that Directly Participate in the Process," *Toxins,* vol. 3, pp. 294-308, 2011.

[14] B. L. Kagan, A. Finkelstein and M. Colombini, "Diphtheria toxin fragment forms large pores in phospholipid bilayer membranes," *Proc. Natl. Acad. Sci.,* vol. 78, no. 8, pp. 4950-4954, 1981.

[15] S. Sun, W. H. Tepp, E. A. Johnson and E. R. Chapman, "Botulinum Neurotoxins B and E Translocate at Different Rates and Exhibit Divergent Responses to GT1b and Low pH," *Biochemistry,* vol. 51, p. 5655−5662, 2012.

[16] T. L. Repella, M. Ho, T. P. Chong, Y. Bannai and B. A. Wilson, "Arf6-Dependent Intracellular Trafficking of Pasteurella multocida Toxin and pH-Dependent Translocation from Late Endosomes," *Toxins,* pp. 218-241, 2011.

[17] S. Contamin, A. Galmiche, A. Doye, G. Flatau, A. Benmerah and P. Boquet, "The p21 Rho-activating Toxin Cytotoxic Necrotizing Factor 1 Is Endocytosed by a Clathrin-independent Mechanism and Enters the Cytosol by an Acidicdependent Membrane Translocation Step," *Molecular Biology of the Cell,* vol. 11, pp. 1775-1787, 2000.

[18] B. Blumenthal, C. Hoffmann, K. Aktories, S. Backert and G. Schmidt, "The Cytotoxic Necrotizing Factors from Yersinia pseudotuberculosis and from Escherichia coli Bind to Different Cellular Receptors but Take the Same Route to the Cytosol," *Infection and Immunity,* vol. 75, no. 7, pp. 3344-3353, 2007.

[19] T. Repella, "Investigation of the Intracellular Trafficking Pathways of the Dermonecrotic Toxin Family," University of Illinois at Urbana-Champaign, Urbana, IL, 2011.

[20] B. Wilson and M. Ho, "Cellular and molecular action of the mitogenic protein-deamidating toxin from Pasteurella multocida," *The FEBS Journal,* p. 4616–4632, 2011.

[21] J. H. C. Orth, I. Preuss, I. Fester, A. Schlosser, B. A. Wilson and K. Aktories, "Pasteurella multocida toxin activation of heterotrimeric G proteins by deamidation," *Proc. Nat. Acad. Sci.,* vol. 106, no. 17, p. 7179–7184, 2009.

[22] J. H. C. Orth, S. Lang, M. Taniguchi and K. Aktories, "Pasteurella multocida Toxin-induced Activation of RhoA Is Mediated via Two Families of Gα Proteins, Gαq and Gα12/13," *The Journal of Biological Chemistry,* vol. 280, no. 44, p. 36701–36707, 2005.

[23] L. Landraud, M. Gauthier, T. Fosse and P. Boquet, "Frequency of Escherichia coli strains producing the cytotoxic necrotizing factor (CNF1) in nosocomial urinary tract infections," *Letters in Applied Microbiology,* no. 30, pp. 213-216, 2000.

[24] M. Mills, K. C. Meysick and A. D. O'Brien, "Cytotoxic Necrotizing Factor Type 1 of Uropathogenic Escherichia coli Kills Cultured Human Uroepithelial 5637 Cells by an Apoptotic Mechanism," *Infection and Immunity,* vol. 68, no. 10, p. 5869–5880, 2000.

[25] S. Pei, A. Doye and P. Boquet, "Mutation of specific acidic residues of the CNF1 T domain into lysine alters cell membrane translocation of the toxin," *Molecular Microbiology,* vol. 41, no. 6, pp. 1237-1247, 2001.

[26] C. Fiorentini, A. Fabbri, G. Flatau, G. Donelli and P. Matarrese, "Escherichia coli Cytotoxic Necrotizing Factor 1 (CNF1), a Toxin That Activates the Rho GTPase," *The Journal of Biological Chemistry,* vol. 272, pp. 19532-19537, 1997.

[27] G. Flatau, E. Lemichez, M. Gauthier, P. Chardin, S. Paris, C. Fiorentini and P. Boquet, "Toxin-induced activatin of the G protein p21 Rho by deamidation of glutamine," *Nature,* vol. 387, pp. 729-736, 1997.

[28] M. Lerm, M. Pop, G. Fritz, K. Aktories and G. Schmidt, "Proteasomal Degradatoin of Cytotoxic Necrotizing Factor 1-Activated Rac," *Infection and Immunity,* vol. 70, no. 8, pp. 4053-4058, 2002.

[29] L. Buetow, G. flatau, K. Chiu, P. Boquet and P. Ghosh, "Structure of the Rho-activating domain of Escherichia coli cytotoxic necrotizing factor 1," *Nature Structural Biology,* vol. 8, no. 7, pp. 584-588, 2001.

[30] G. Schmidt, J. Selzer, M. Lerm and K. Aktories, "The Rho-deamidating Cytotoxic Necrotizing Factor 1 from Escherichia coli Possesses Transglutaminase Activity," *The Journal of Biological Chemistry,* 1998.

[31] H. A. Lockman, R. A. Gillespie, B. D. Baker and E. Shakhnovich, "Yersinia pseudotuberculosis Produces a Cytotoxic Necrotizing Factor," *Infection and Immunity,* vol. 70, no. 5, pp. 2708-2714, 2002.

[32] C. Hoffmann, M. Pop, J. Leemhuis, J. Schirmer and K. Aktories, "The Yersinia pseudotuberculosis Cytotoxic Necrotizing Factor (CNFY) Selectively Activates RhoA," *The Journal of Biological Chemistry,* vol. 279, no. 16, pp. 16026-16032, 2004.

[33] M. Ho, L.-H. Chang, M. Pires-Alves, B. Thyagarajan, J. E. Bloom, Z. Gu, K. K. Aberle, S. A. Teymorian, Y. Bannai, S. C. Johnson, J. J. McArdle and B. A. Wilson, "Recombinant botulinum neurotoxin A heavy chain-based delivery vehicles for neuronal cell targeting," *Protein Engineering, Design & Selection,* vol. 24, no. 3, pp. 247-253, 2010.

[34] H. Inoue, H. Nojima and H. Okayama, "High efficiency transformation of Escherichia coli with plasmids," *Gene,* pp. 23-28, 1990.

[35] M. goujon, H. McWilliam, W. Li, F. Valentin, S. Squizzato, J. Paern and R. Lopez, "A new bioinformatics analysis tools framework at EMBL-EBI," *Nucleic Acids Research,* vol. 38, p. 695–699, 2010.

[36] M. Larkin, G. Blackshields, N. Brown, R. Chenna, P. McGettigan, H. McWilliam, F. Valentin, I. Wallace, A. Wilm, R. Lopez, J. Thompson, T. Gibson and D. Higgins, "Clustal W and Clustal X version 2.0," *Bioinformatics,* vol. 23, no. 21, p. 2947–2948, 2007.

[37] W. R. Pearson and D. J. Lipman, "Improved tools for biological sequence comparison," *Proc. Natl. Acad. Sci.,* vol. 85, pp. 2444-2448, 1988.